Detecting ultra-light particles from astrophysical observations

Y-f. Chen, J. Shu., X. Xiao, Q. Yuan, Y. Zhao,
arxiv: 1905.02213 (accepted in Phys.Rev.Lett.)

H-k. Guo, Y-q. Ma, J. Shu., X. Xiao, Q. Yuan, Y. Zhao,
arxiv: 1902.05962 JCAP 1905 (2019) 015

J. Shu., X. Xiao, Z-j. Xia, Q. Yuan, Y. Zhao, X-j. Zhu, with PPTA collaboration, in preparation

Outline

- Introduction
- Probing DPDM from Gaia (Position/velocity)
- Probing DPDM from Gaia (Time)
- EHT polarmetric measurements on axion cloud from SMBH
- Summary

High energy physics

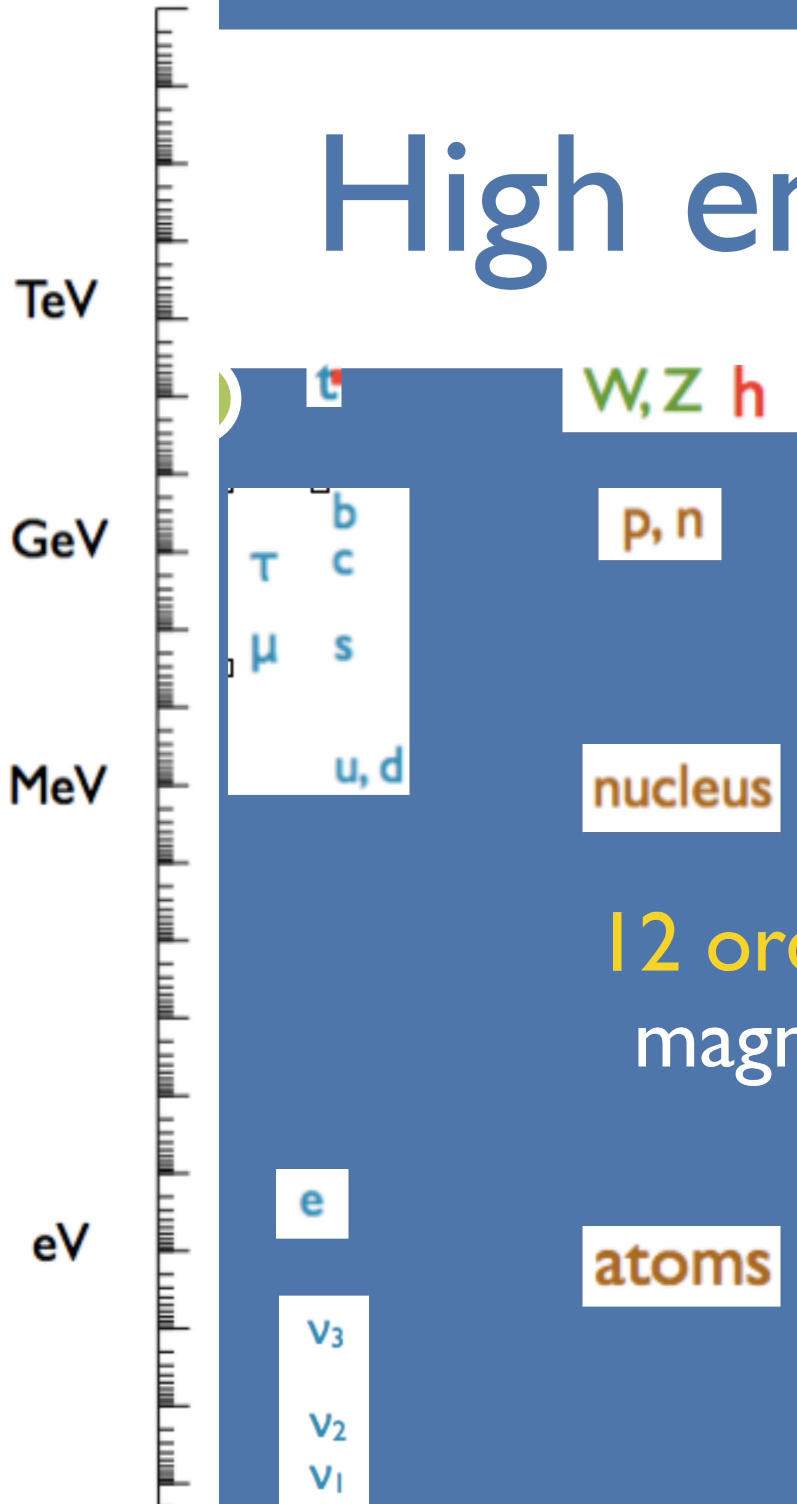

2012

Higher and higher energy

12 orders of magnitude

Last 122 years

Extremely successful!

1895

Open the door of sub-atom physics

Not just higher energy

Besides the higher and higher energies, we may consider other extreme environment to search for NP

neutrino physics

high energy cosmic rays/neutrinos

Flavor physics

LHC colliders

Super light particles (QCD, axion, ALPs, DP, ….)

Table top exp: Cavity, LC circult, quantum sensor, etc.

Astrophysical exp: Radio signal, sun, GWs, supernova, etc.

Probing DPDM through Gaia

H-k. Guo, Y-q. Ma, J. Shu., X. Xiao, Q. Yuan, Y. Zhao,
arxiv: 1902.05962 JCAP 1905 (2019) 015

Ultra-light DM

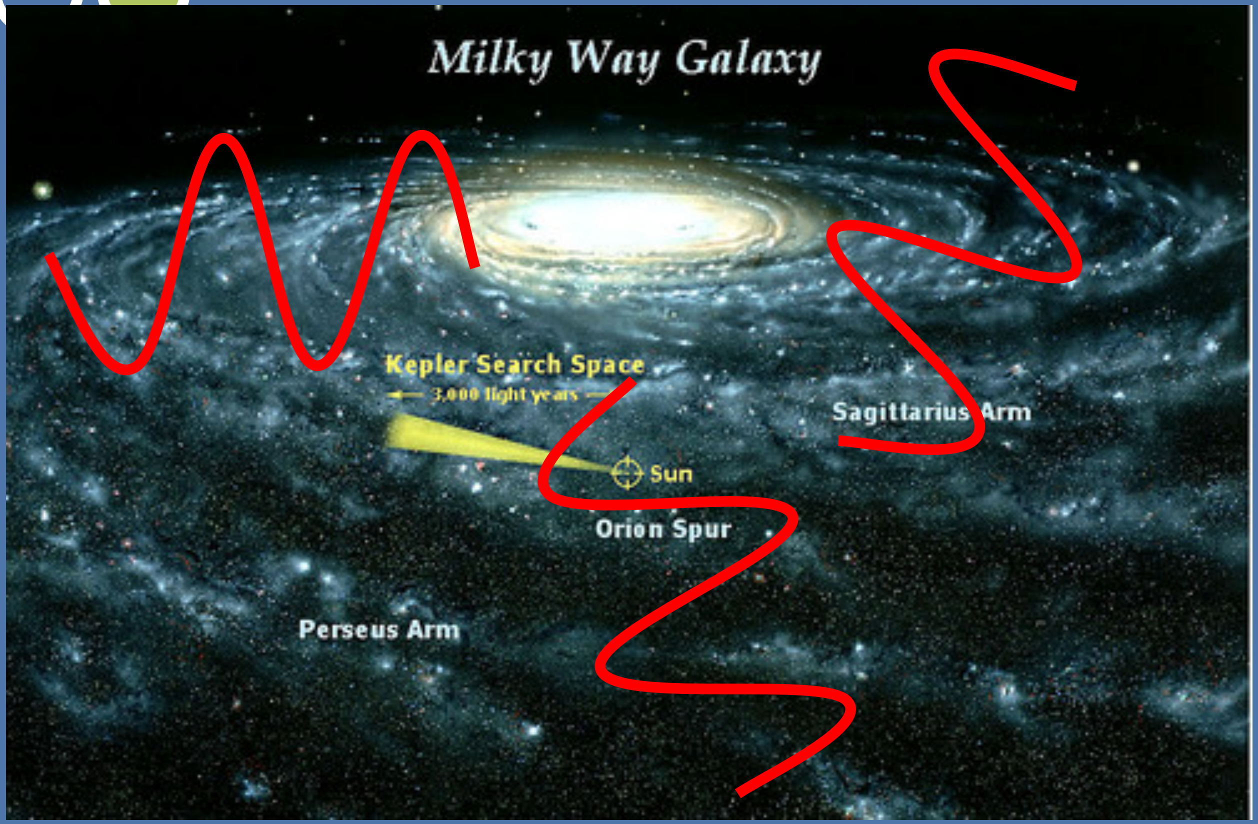

Difficult to detect, need astrophysical observations.

For ultra-light DM(~10^{-22} eV), they form super low frequency (nHz) oscillating backgrounds

Fussy DM

Excellent ultralight DM candidate

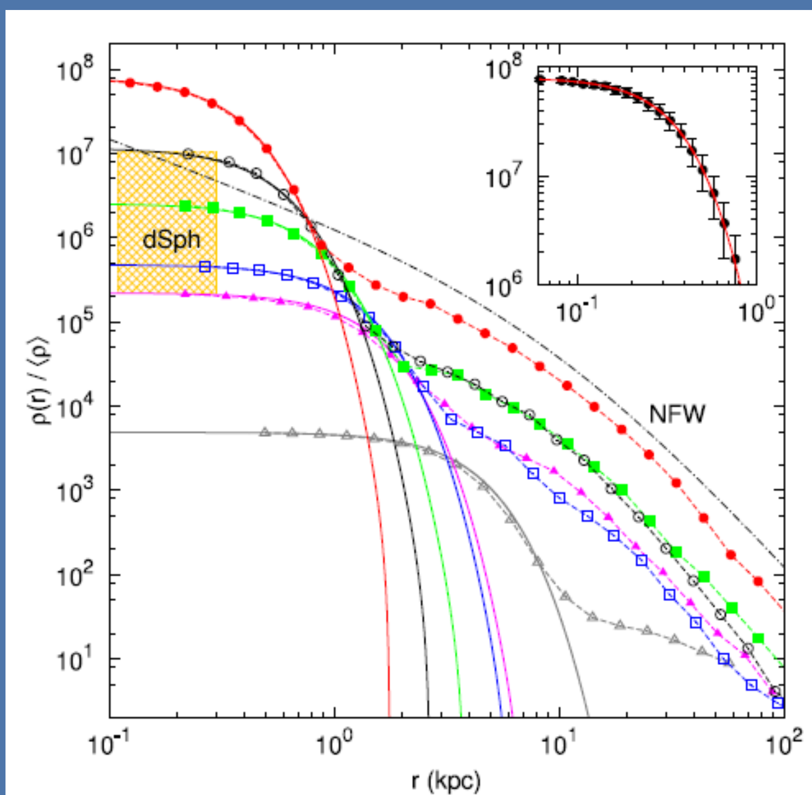

Ultra-light bosonic DM can cause BEC, and behave like CDM at large scale

At small scale (comparing to wavelength, m~10^{-22} eV, λ~kpc), it can be used to solve the cusp-core problem

Hu et al., 2000

Ultralight DM is expected to have a soliton core

$$\rho(x) = \begin{cases} 0.019\left(\frac{m_a}{m_{a,0}}\right)^{-2}\left(\frac{l_c}{1\mathrm{kpc}}\right)^{-4} M_\odot \mathrm{pc}^{-3}, & \text{for } r < l_c \\ \frac{\rho_0}{r/R_H(1+r/R_H)^2}, & \text{for } r > l_c \end{cases}$$

soliton solution

NFW profile

Ultra-light DPDM

A hypothetical hidden-sector particle proposed as a force carrier similar to photon

Considering a special class of dark photon which is the gauge boson of the $U(1)_B$ or $U(1)_{B-L}$ group: it would interact with any object with B or (B-L) number (“dark charge”)

A good candidate of (fuzzy) dark matter (DPDM)

If its is very small (10^{-22} eV), the dark photon behaves like an oscillating background, drives displacements for particles with “dark charge”

Precision of star position

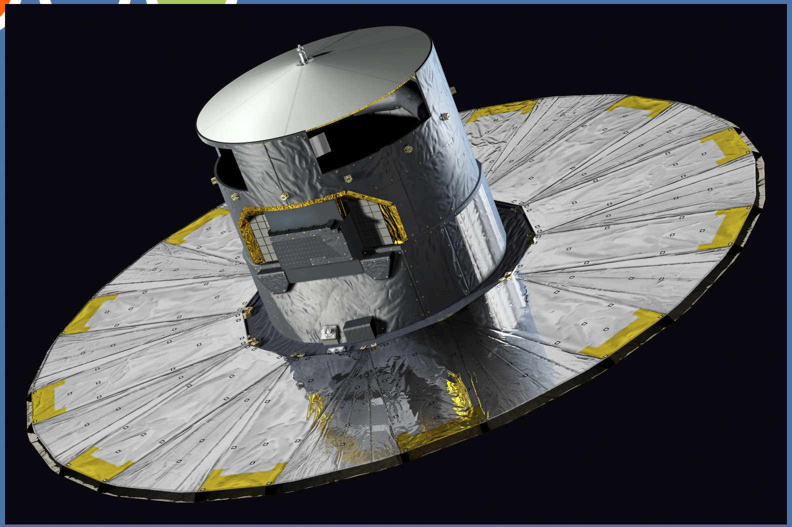

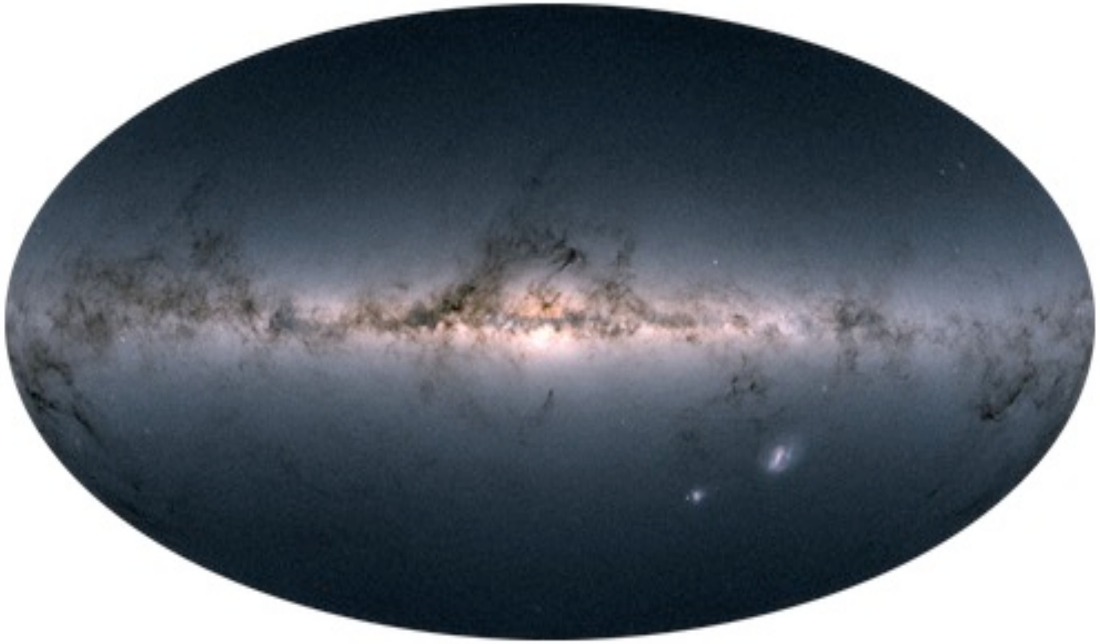

Gaia satelite (2003), plan to accurately measure 1% of star inside the Milky Way (~10^9) for their position and speed.

Expect breakthrough in the Milky Way structure, evolution of stars, new planet, fundamental physics, etc.

Aberration of Light

Objects(Gaia statelite) feel an oscillating acceleration in the DPDM backgrounds

$$\boldsymbol{a}(t,\boldsymbol{x}) \simeq \epsilon e \frac{q}{m} m_A \boldsymbol{A_0} \cos(m_A t - \boldsymbol{k}\cdot\boldsymbol{x})$$

This acceleration will cost the velocity has a periodic change, therefore periodically shift the position of the star from the observer

$$\Delta \boldsymbol{v}(t,\boldsymbol{x}) \simeq \epsilon e \frac{q}{m} \boldsymbol{A_0} \sin(m_A t - \boldsymbol{k}\cdot\boldsymbol{x}).$$

$$\Delta\theta \simeq -\Delta v \sin\theta$$

radial direction not very accurate

A large sample of the star position period variation will hint the signal.

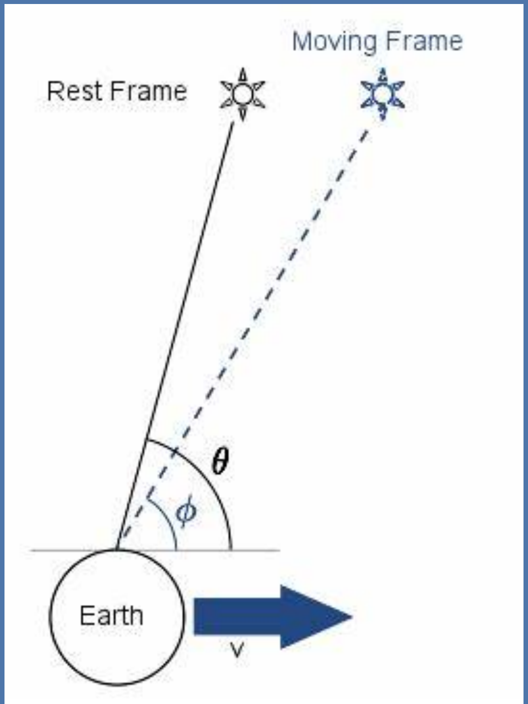

Gaia search for ultra-light DPDM

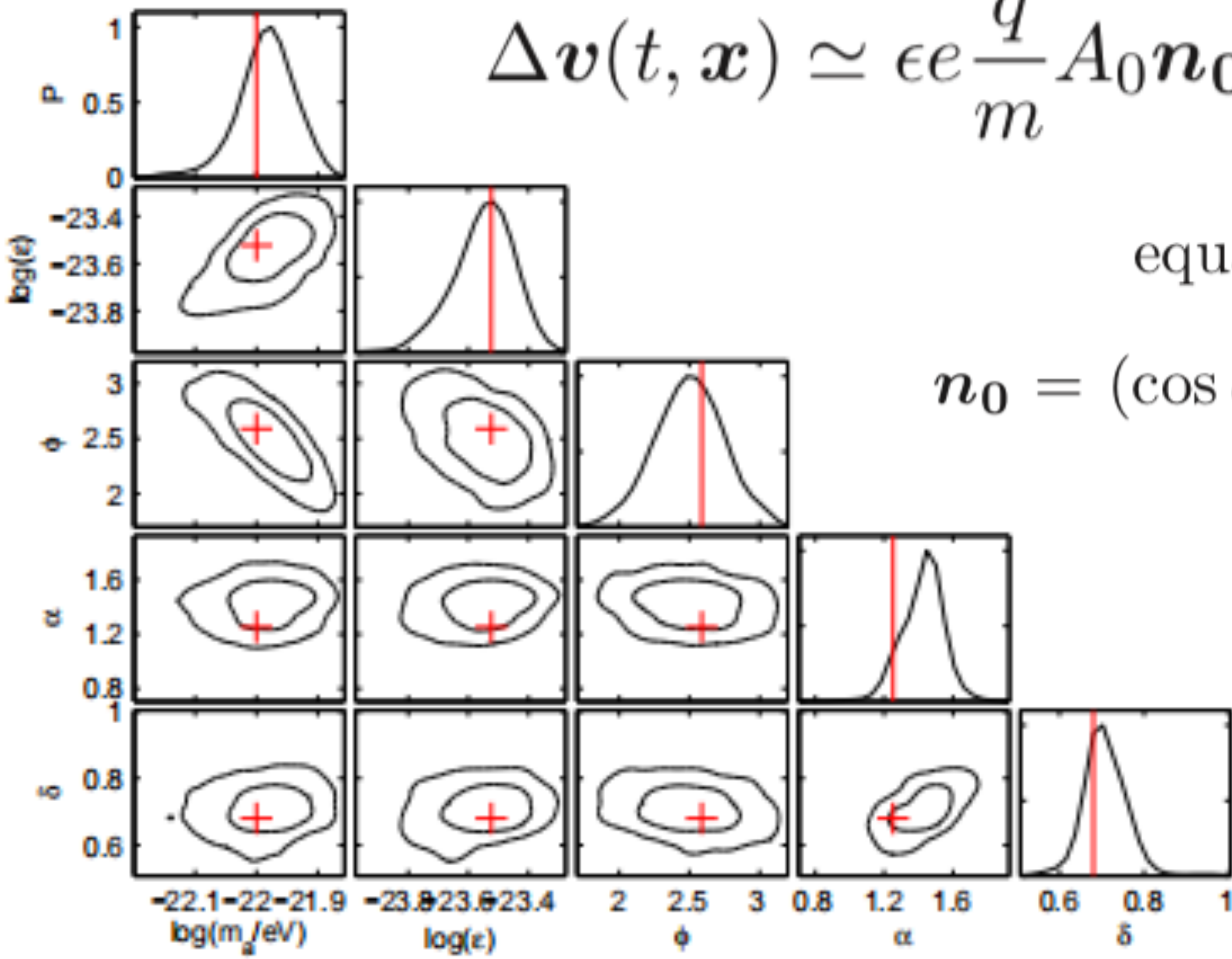

$$\Delta \boldsymbol{v}(t, \boldsymbol{x}) \simeq \epsilon e \frac{q}{m} A_0 \boldsymbol{n_0} \sin[m_A(t - t_0) + \phi],$$

equatorial coordinate (α, δ)

$$\boldsymbol{n_0} = (\cos\delta\cos\alpha,\ \cos\delta\sin\alpha,\ \sin\delta),$$

Compressed data, high accretion

$$\sigma = 100\ \mu\mathrm{as}/\sqrt{10^5}.$$

mock data

$$(m_A, \epsilon, \phi, \alpha, \delta) = (10^{-22}\ \mathrm{eV}, 3 \times 10^{-24}, 2.59, 1.25, 0.68).$$

Gaia search for ultra-light DPDM

95% C.L. exclusion by varing mass and coupling constant

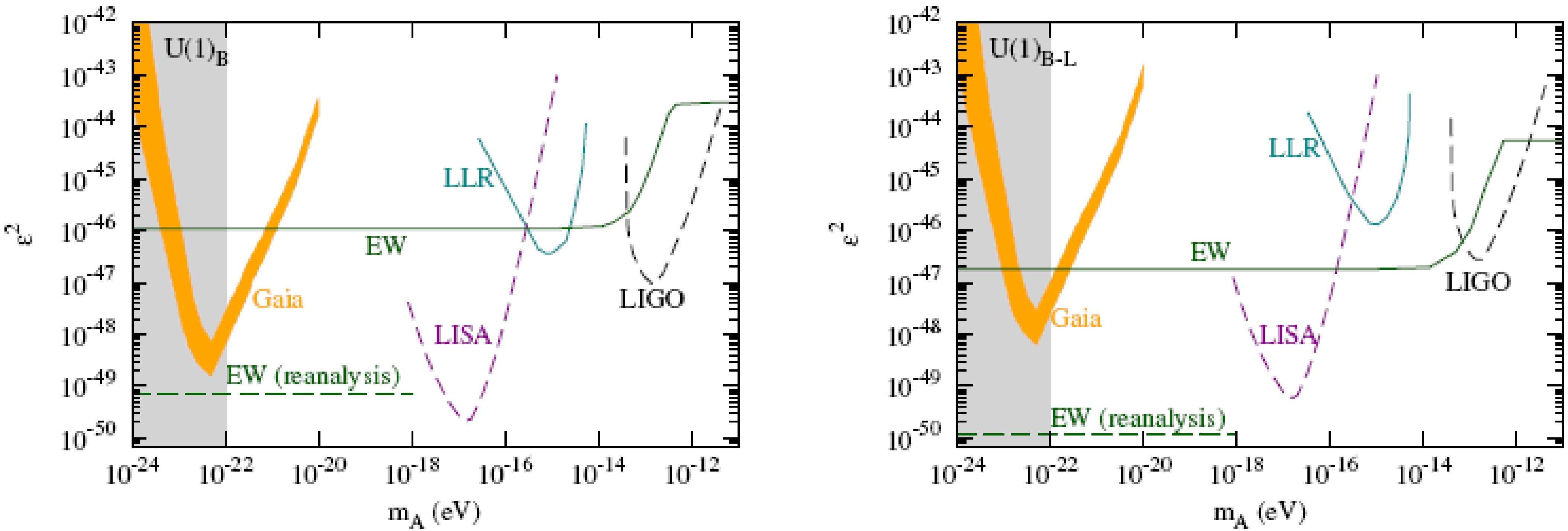

Future Gaia final data release will give you the real data with time sequence

Probing DPDM through PTA

J. Shu., X. Xiao, Z-j. Xia, Q. Yuan, Y. Zhao, X-j. Zhu, with PPTA collaboration, in preparation

The pulsar timing array (PTA)

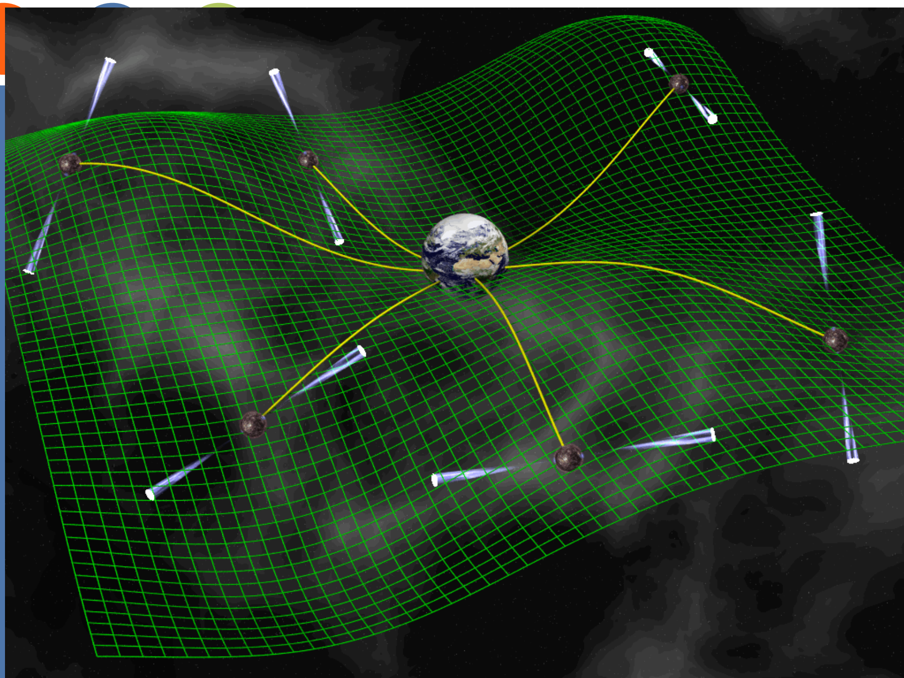

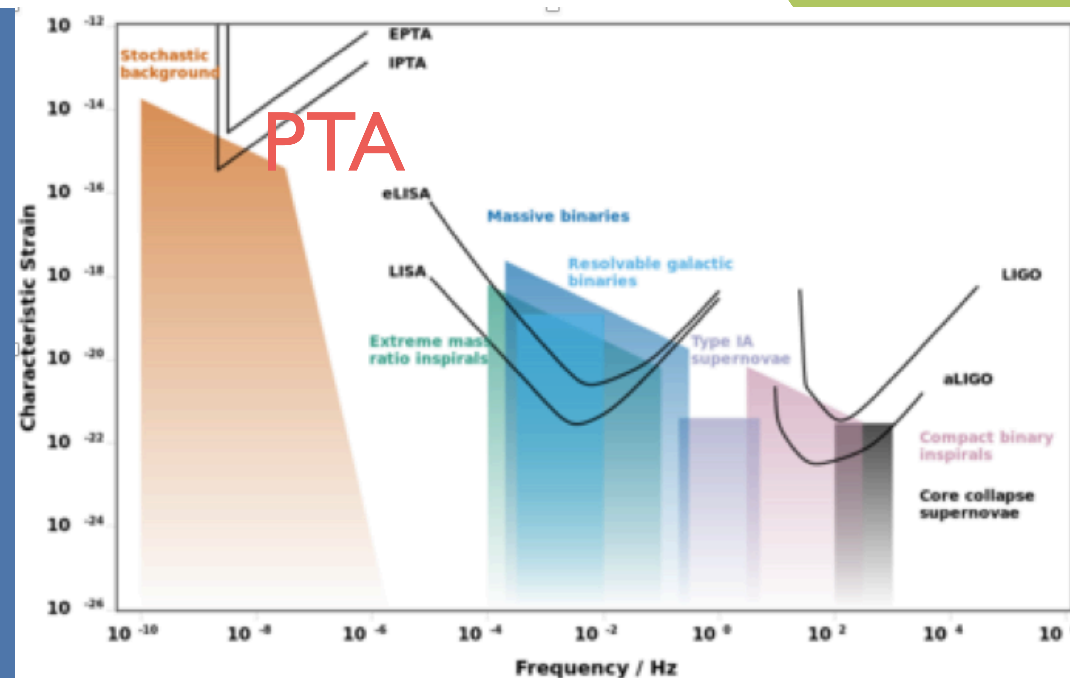

mili-seconds pulsar is the stablest “clock” in cosmology.

accurately measure the change of the time pulse can be used to probe nHz gravitational waves

Can be used to probe other fundamental physics like DM

Sensitivity of GW search from NANOGrav PTA

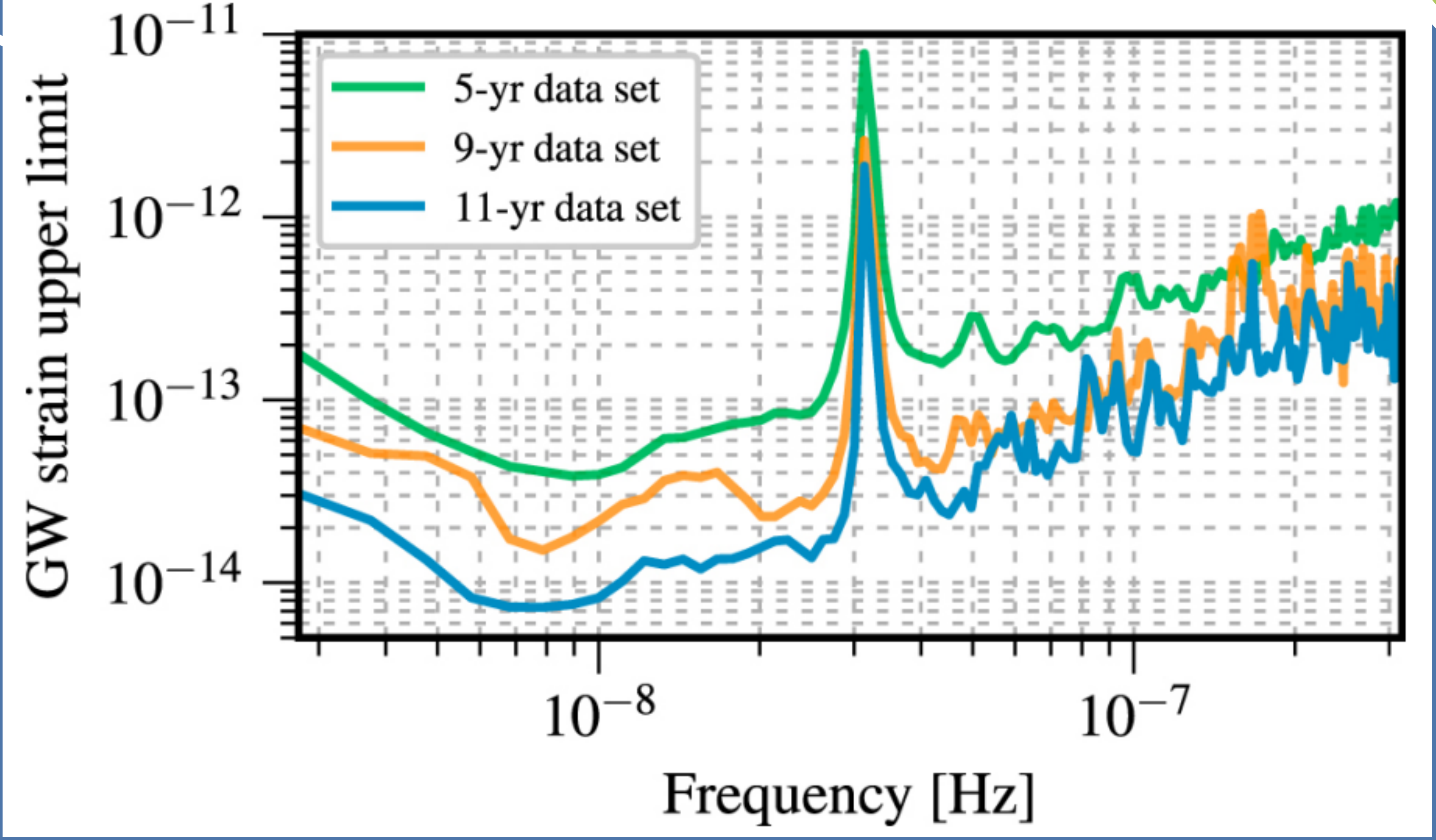

Aggarwal et al. (2019)

Use PTA to probe Ultra-light DPDM

Earth and pulsars are in the oscillating DPDM background, will cause an oscillating shift for the pulse

$$\delta \boldsymbol{x}_{e,p}(t) \simeq -\frac{\epsilon e q}{m_A m} \boldsymbol{A_0}^{e,p} \cos\left[m_A(t-t_0)+\alpha_{e,p}\right]$$

$$\Delta t_r^d(t) = \frac{\left|\boldsymbol{d}+\delta \boldsymbol{x}_p\left(t-\frac{|\boldsymbol{d}|}{v(t)}\right)-\delta \boldsymbol{x}_e(t)\right|-|\boldsymbol{d}|}{v(t)} \simeq \frac{\boldsymbol{n}_p \cdot \Delta \boldsymbol{x}(t)}{v(t)},$$

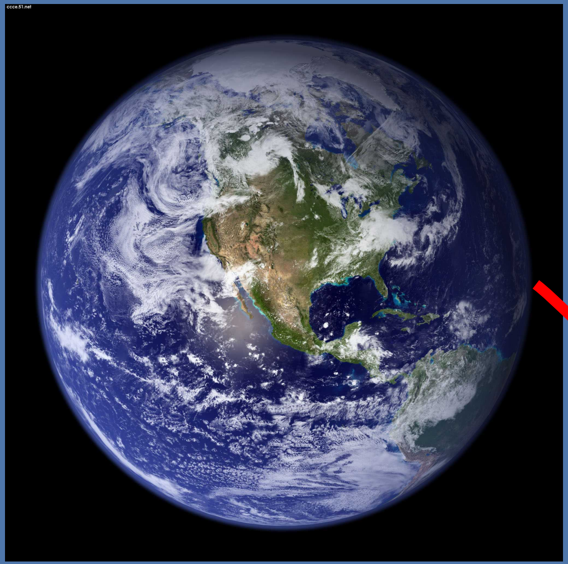

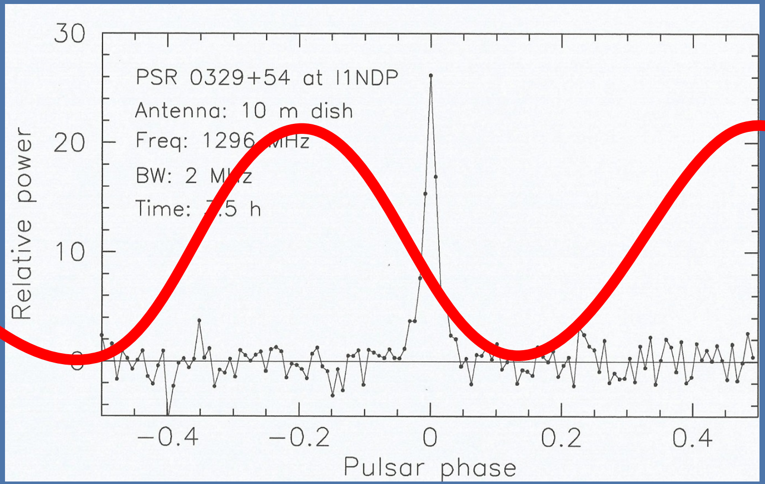

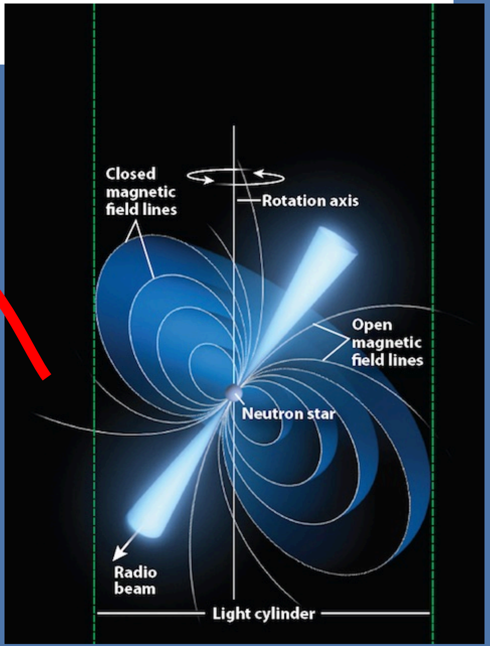

Parkes PTA数据

64m Parkes telescope in Australia

Pulsars	N_{obs}	T(years)	$\overline{\sigma} \times 10^{-6}(s)$	$\log_{10} A_{SN}$	γ_{SN}	$\log_{10} A_{DM}$	γ_{DM}
J0437-4715	29262	15.03	0.296	$-15.76^{+0.17}_{-0.18}$	$6.63^{+0.17}_{-0.13}$	$-13.05^{+0.10}_{-0.08}$	$2.26^{+0.32}_{-0.44}$
J0613-0200	5920	14.20	2.504	$-14.63^{+0.77}_{-0.68}$	$4.93^{+1.33}_{-1.61}$	$-13.02^{+0.08}_{-0.08}$	$0.95^{+0.33}_{-0.31}$
J0711-6830	5547	14.21	6.197	$-12.85^{+0.14}_{-0.16}$	$0.97^{+0.64}_{-0.55}$	$-14.54^{+0.72}_{-0.89}$	$4.43^{+1.68}_{-1.72}$
J1017-7156	4053	7.77	1.577	$-12.89^{+0.07}_{-0.07}$	$0.54^{+0.53}_{-0.37}$	$-12.72^{+0.06}_{-0.06}$	$2.18^{+0.45}_{-0.44}$
J1022+1001	7656	14.20	5.514	$-12.79^{+0.12}_{-0.13}$	$0.54^{+0.55}_{-0.37}$	$-13.04^{+0.10}_{-0.12}$	$0.58^{+0.47}_{-0.36}$
J1024-0719	2643	14.09	4.361	$-14.28^{+0.27}_{-0.20}$	$6.51^{+0.35}_{-0.60}$	$-14.53^{+0.54}_{-0.56}$	$5.22^{+1.14}_{-1.18}$
J1045-4509	5611	14.15	9.186	$-12.75^{+0.24}_{-0.40}$	$1.58^{+1.28}_{-0.93}$	$-12.18^{+0.09}_{-0.08}$	$1.86^{+0.36}_{-0.32}$
J1125-6014	1407	12.34	1.981	$-12.64^{+0.11}_{-0.12}$	$0.51^{+0.55}_{-0.37}$	$-13.14^{+0.19}_{-0.21}$	$3.36^{+0.73}_{-0.66}$
J1446-4701	508	7.36	2.200	$-16.46^{+2.88}_{-3.17}$	$2.74^{+2.49}_{-1.89}$	$-13.49^{+0.32}_{-1.87}$	$2.48^{+1.92}_{-1.45}$
J1545-4550	1634	6.97	2.249	$-17.33^{+2.50}_{-2.55}$	$3.25^{+2.45}_{-2.18}$	$-13.40^{+0.24}_{-0.38}$	$3.90^{+1.61}_{-1.09}$
J1600-3053	7047	14.21	2.216	$-17.63^{+2.10}_{-2.29}$	$3.28^{+2.34}_{-2.15}$	$-13.27^{+0.12}_{-0.13}$	$2.79^{+0.43}_{-0.40}$
J1603-7202	5347	14.21	4.947	$-12.82^{+0.14}_{-0.16}$	$1.01^{+0.67}_{-0.60}$	$-12.66^{+0.10}_{-0.09}$	$1.44^{+0.40}_{-0.38}$
J1643-1224	5941	14.21	4.039	$-12.32^{+0.08}_{-0.09}$	$0.51^{+0.42}_{-0.34}$	$-12.27^{+0.07}_{-0.07}$	$0.55^{+0.32}_{-0.29}$
J1713+0747	7804	14.21	1.601	$-14.09^{+0.25}_{-0.38}$	$2.98^{+1.00}_{-0.64}$	$-13.35^{+0.08}_{-0.08}$	$0.53^{+0.32}_{-0.31}$
J1730-2304	4549	14.21	5.657	$-17.39^{+2.39}_{-2.51}$	$3.05^{+2.59}_{-2.12}$	$-14.11^{+0.40}_{-0.57}$	$4.22^{+1.42}_{-1.04}$
J1732-5049	807	7.23	7.031	$-16.51^{+3.04}_{-2.97}$	$3.29^{+2.37}_{-2.97}$	$-13.38^{+0.54}_{-0.84}$	$4.07^{+1.96}_{-1.93}$
J1744-1134	6717	14.21	2.251	$-13.39^{+0.14}_{-0.15}$	$1.49^{+0.66}_{-0.57}$	$-13.35^{+0.09}_{-0.09}$	$0.86^{+0.40}_{-0.33}$
J1824-2452A	2626	13.80	2.190	$-12.56^{+0.13}_{-0.12}$	$3.61^{+0.41}_{-0.39}$	$-12.18^{+0.11}_{-0.10}$	$1.64^{+0.46}_{-0.59}$
J1832-0836	326	5.40	1.430	$-16.47^{+2.63}_{-3.09}$	$3.66^{+2.33}_{-2.52}$	$-13.07^{+0.24}_{-0.63}$	$3.77^{+2.00}_{-1.05}$
J1857+0943	3840	14.21	5.564	$-14.76^{+0.74}_{-0.50}$	$5.75^{+0.91}_{-1.53}$	$-13.40^{+0.20}_{-0.25}$	$2.66^{+0.83}_{-0.67}$
J1909-3744	14627	14.21	0.672	$-13.60^{+0.13}_{-0.12}$	$1.60^{+0.43}_{-0.46}$	$-13.48^{+0.09}_{-0.08}$	$0.69^{+0.38}_{-0.35}$
J1939+2134	4941	14.09	0.468	$-14.38^{+0.22}_{-0.18}$	$6.24^{+0.49}_{-0.62}$	$-11.59^{+0.07}_{-0.07}$	$0.13^{+0.19}_{-0.10}$
J2124-3358	4941	14.21	8.863	$-14.79^{+0.82}_{-0.67}$	$5.07^{+1.37}_{-1.97}$	$-13.35^{+0.18}_{-0.33}$	$0.95^{+1.11}_{-0.66}$
J2129-5721	2879	13.88	3.496	$-15.48^{+1.92}_{-3.54}$	$2.91^{+2.29}_{-1.83}$	$-13.31^{+0.13}_{-0.14}$	$1.07^{+0.65}_{-0.65}$
J2145-0750	6867	14.09	5.086	$-12.82^{+0.10}_{-0.11}$	$0.62^{+0.50}_{-0.40}$	$-13.33^{+0.14}_{-0.16}$	$1.38^{+0.54}_{-0.55}$
J2241-5236	5224	8.20	0.830	$-13.40^{+0.09}_{-0.08}$	$0.44^{+0.40}_{-0.30}$	$-13.79^{+0.10}_{-0.10}$	$1.42^{+0.61}_{-0.59}$

脉冲到达时间（TOA）

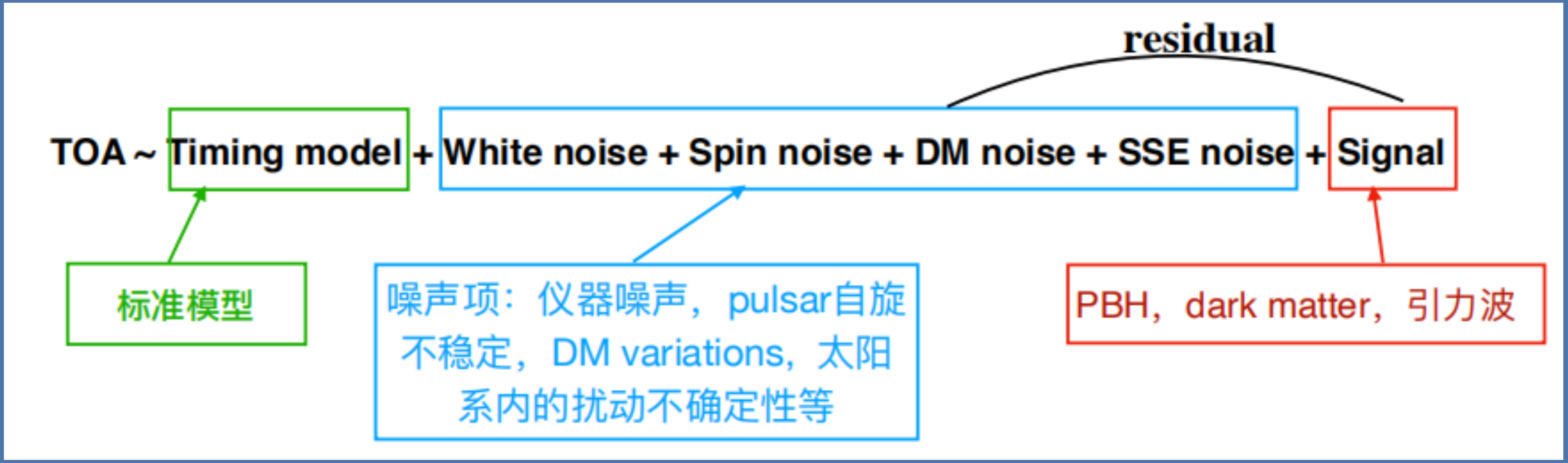
residual
TOA ~ Timing model + White noise + Spin noise + DM noise + SSE noise + Signal
标准模型
噪声项：仪器噪声，pulsar自旋不稳定，DM variations，太阳系内的扰动不确定性等
PBH，dark matter，引力波

Pulsar Modeling

```
PSRJ           J0030+0451
RAJ             00:30:27.4299630         1  0.00000000083327092134
DECJ           +04:51:39.75230           1  0.00000000193016085164
F0             205.53069608827312545     1  1.6735454617113885805e-13
F1             -4.3060388399134177208e-16 1  2.0847319452591396919e-21
PEPOCH         53000
POSEPOCH       53000
DMEPOCH        53000
PMRA           -4.0541352583640798551    1  0.06006537664217530270
PMDEC          -5.0337686500180439013    1  0.14002511698705866205
PX             4.0229124332613435578     1  0.02065704842394362750
EPHVER         5
CLK            UNCORR
MODE 1
EPHEM          DE414
DM             1 1 0
DM1            0 1 0
DM2            0 1 0
```

Right ascension, RA (J2000)
Declination, DEC (J2000)
Proper motion in RA (mas yr^{-1})
Proper motion in DEC (mas yr^{-1})
Spin frequency, f (s^{-1})
$\dot{f}$ (s^{-2})
Parallax, π (mas)
Dispersion measure, DM (cm^{-3} pc)
$\dot{DM}$ (cm^{-3} pc yr^{-1})
$\ddot{DM}$ (cm^{-3} pc yr^{-2})

Binary model
Orbital period, P_b (d)
Epoch of periastron, T_0 (MJD)
Projected semi-major axis, x (lt-s)
Longitude of periastron, ω_0 (deg)
Eccentricity, e
Sine of inclination, $\sin i$
Companion mass, m_c ($M_\odot$)
Derivative of P_b, $\dot{P}_b$
Periastron advance $\dot{\omega}_0$ (deg yr^{-1})
Epoch of ascending node, T_{asc} (MJD)

Noise Model

White noise (irrelevant to signal)： from device、pulsar timing templet

Red noise （relevant）： pulsar rotation noise、from propagation

Turbulence in the solar system： from big planet, etc

Noise from target sources： plasma cloud between pulsar and earth

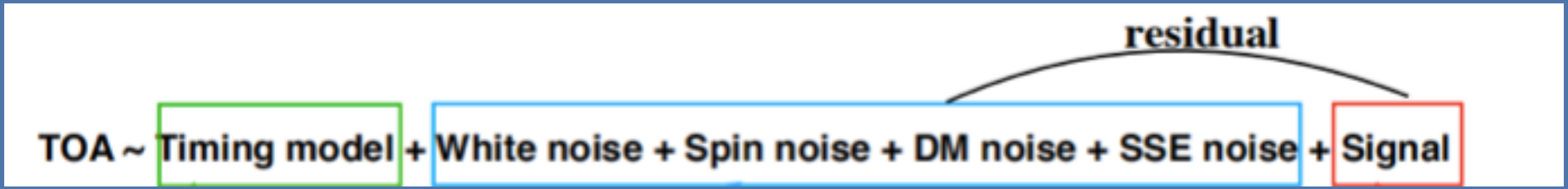

Parkes PTA preliminary

fully correlated (lower) or uncorrelated (upper) DPDM polarization

pulsar: 0.2~2kpc

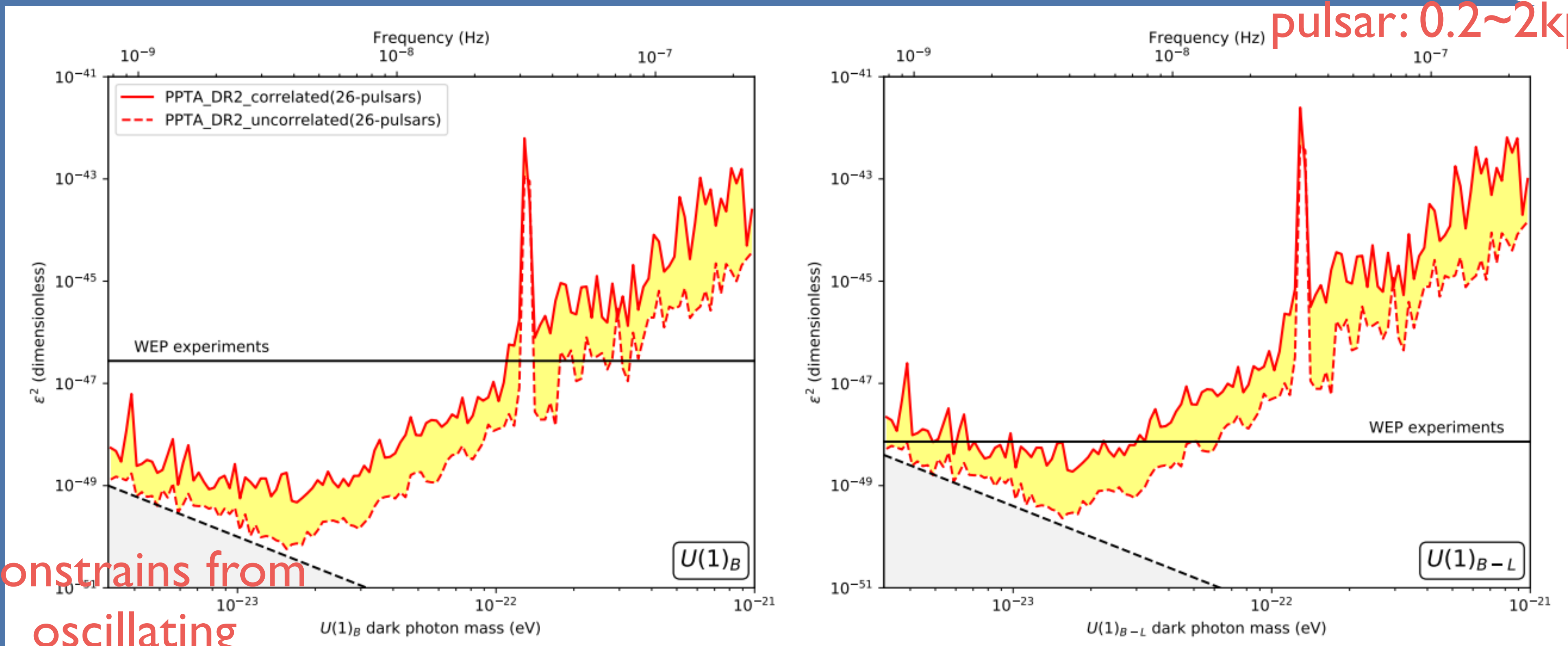

Constrains from oscillating gravitational potential

revolution around the sun (periodic signal)

Will be the best in the world for certain mass range

Probing Axions with Event Horizon Telescope Polarimetric Measurements

Y-f. Chen, J. Shu., X. Xiao, Q. Yuan, Y. Zhao,
arxiv: 1905.02213 (accepted in Phys.Rev.Lett.)

Theory motivation

Strong CP problem

$$\underbrace{(\Theta - \arg\det M_q)}_{-\pi \le \bar{\Theta} \le +\pi} \frac{\alpha_s}{8\pi} G\tilde{G}$$

<10^{-11}

Induced axion fields

misalignment

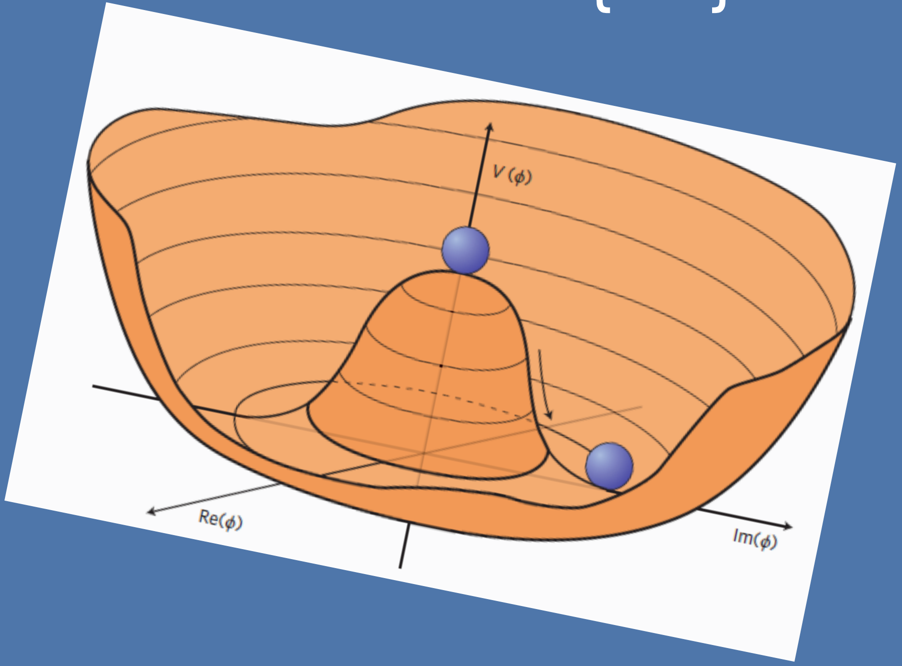

PQ symmetry soft explicit
broken at high scale f

pNGB naturally very light

Why axion?

Big problems of particle physics & Comoslogy

- Strong CP problem
- The identity of dark matter — misalignment mechanism, non-thermal DM
- Gauge hierarchy problem, the origin of EWSB — relaxion
- Baryogenesis
- Inflation
- Cosmological Constant Problem

Search of axion

How to search axion?

Axion-couplings:

- Axion-photon

  ADMX

  CAST

  LIGO, pulsar, etc

- Axion-gluon

  QCD phase transition

  CASPEr

  Many other observations, etc

Axion like particle

Axion induce birefringent effect:

$$\mathcal{L} = -\frac{1}{4}F_{\mu\nu}F^{\mu\nu} - \frac{1}{2}g_{a\gamma}aF_{\mu\nu}\tilde{F}^{\mu\nu} + \frac{1}{2}\nabla^{\mu}a\nabla_{\mu}a - V(a),$$

The condensation of a CP-odd particle distinguishes +/-helicities of a photon

$$\nabla\cdot\boldsymbol{E} = g\nabla\varphi\cdot\boldsymbol{B}, \quad \nabla\times\boldsymbol{E} + \frac{\partial\boldsymbol{B}}{\partial t} = 0,$$

$$\nabla\times\boldsymbol{B} - \frac{\partial\boldsymbol{E}}{\partial t} = g\left(\boldsymbol{E}\times\nabla\varphi - \boldsymbol{B}\frac{\partial\varphi}{\partial t}\right),$$

$$\nabla\cdot\boldsymbol{B} = 0,$$

$$\Box\varphi = \frac{\partial^2\varphi}{\partial t^2} - \nabla^2\varphi = -g\boldsymbol{E}\cdot\boldsymbol{B}.$$

Maxell equation
with axion source

Birefringent effect

Axion induced birefringent effect

$$\Box A_{\pm} = \pm 2 i g_{a\gamma} [\partial_z a \dot{A}_{\pm} - \dot{a} \partial_z A_{\pm}],$$

$$\omega_{\pm} \approx k \pm \tfrac{1}{2} g \left(\frac{\partial \varphi}{\partial t} + \nabla \varphi \cdot \frac{\boldsymbol{k}}{k} \right)$$

different phase velocities for +/- helicities

For linearly polarized photons

$$\begin{aligned} \Delta\Theta &= g_{a\gamma} \Delta a(t_{\rm obs}, \mathbf{x}_{\rm obs}; t_{\rm emit}, \mathbf{x}_{\rm emit}) \\ &= g_{a\gamma} \int_{\rm emit}^{\rm obs} ds\, n^{\mu}\, \partial_{\mu} a \\ &= g_{a\gamma} [a(t_{\rm obs}, \mathbf{x}_{\rm obs}) - a(t_{\rm emit}, \mathbf{x}_{\rm emit})], \end{aligned}$$

Measure the change of the position angle:

Requires polarimetric measurements

Event Horizon Telescope

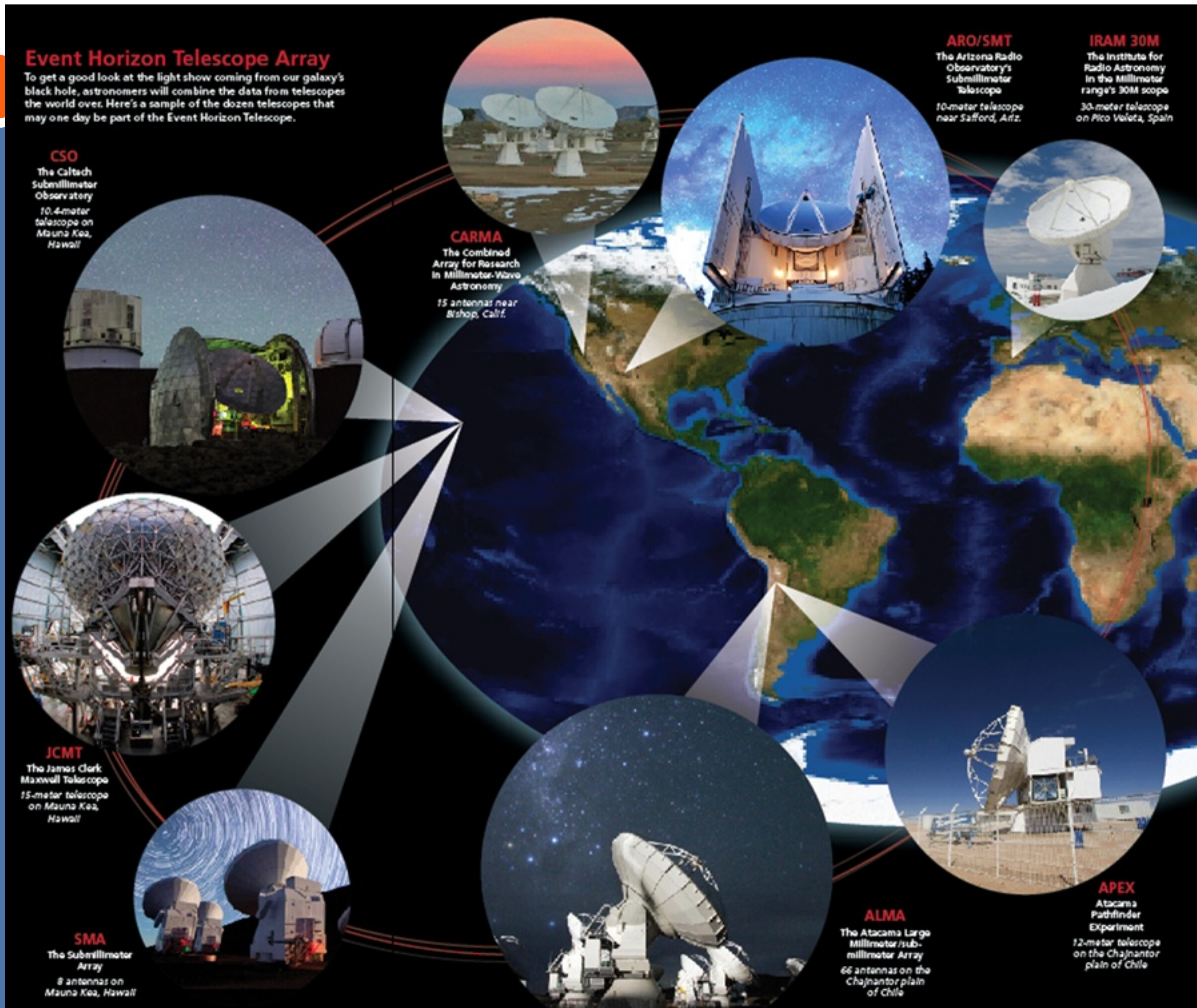

mm telescope array at radio frequency around the Earth

mm wavelength radio telescope particularly good for astro-astro-polarimetric measurements

Farady rotation: position angle around O(1)

Imagine of M87*

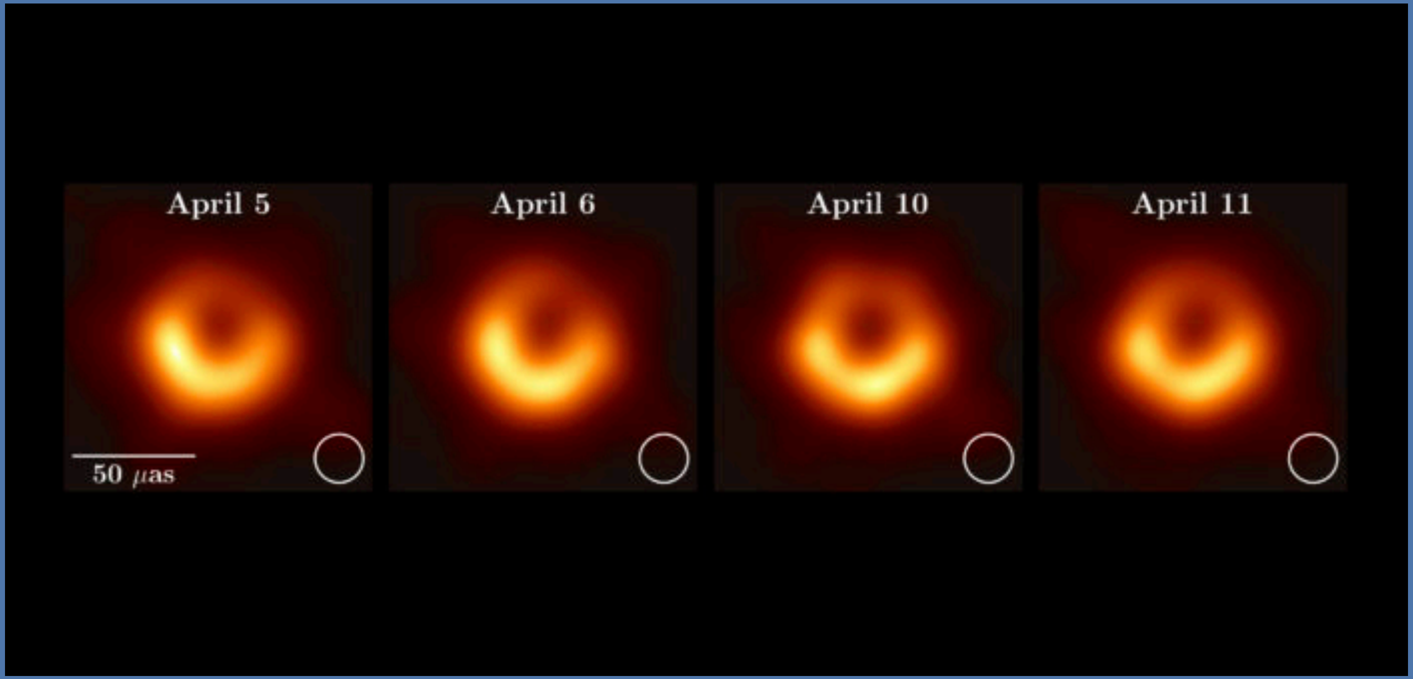

Image of the supermassive black hole at the center of the elliptical galaxy M87, for four different days.

The imagine of the ring is around 5 horizon distance

BH measured and EHT

M87*: 16 Mpc, 10^9 solar mass
10^13 m, 10^-20 eV
10^5 s, a=0.99

Blackhole measured:

Sgr A*: 8 kpc, 10^6 solar mass
10^10 m, 10^-17 eV
100 s, a=?

Excellent anglar resolutions:

20 micro as

resolve features: smaller than BH size (1/3?)

SMBH	M	a_J	μ range	μ for $\alpha = 0.4$	τ_a	τ_{SR}
M87*	$6.5 \times 10^9 M_\odot$	0.99	$2.1 \times (10^{-21} \sim 10^{-20})$ eV	8.2×10^{-21} eV	5.0×10^5 s	$> 1.5 \times 10^{12}$s
Sgr A*	$4.3 \times 10^6 M_\odot$	—	$3.1 \times (10^{-18} \sim 10^{-17})$ eV	1.2×10^{-17} eV	3.3×10^2 s	$> 1.0 \times 10^9$s

TABLE I: Typical parameters of the axion superradiance of the two SMBHs, M87* and Sgr A*.

More on EHT measurements

- Accretion disk around SMBH gives linearly polarized radiation
- Millimeter wavelength: optimal for position angle measurements

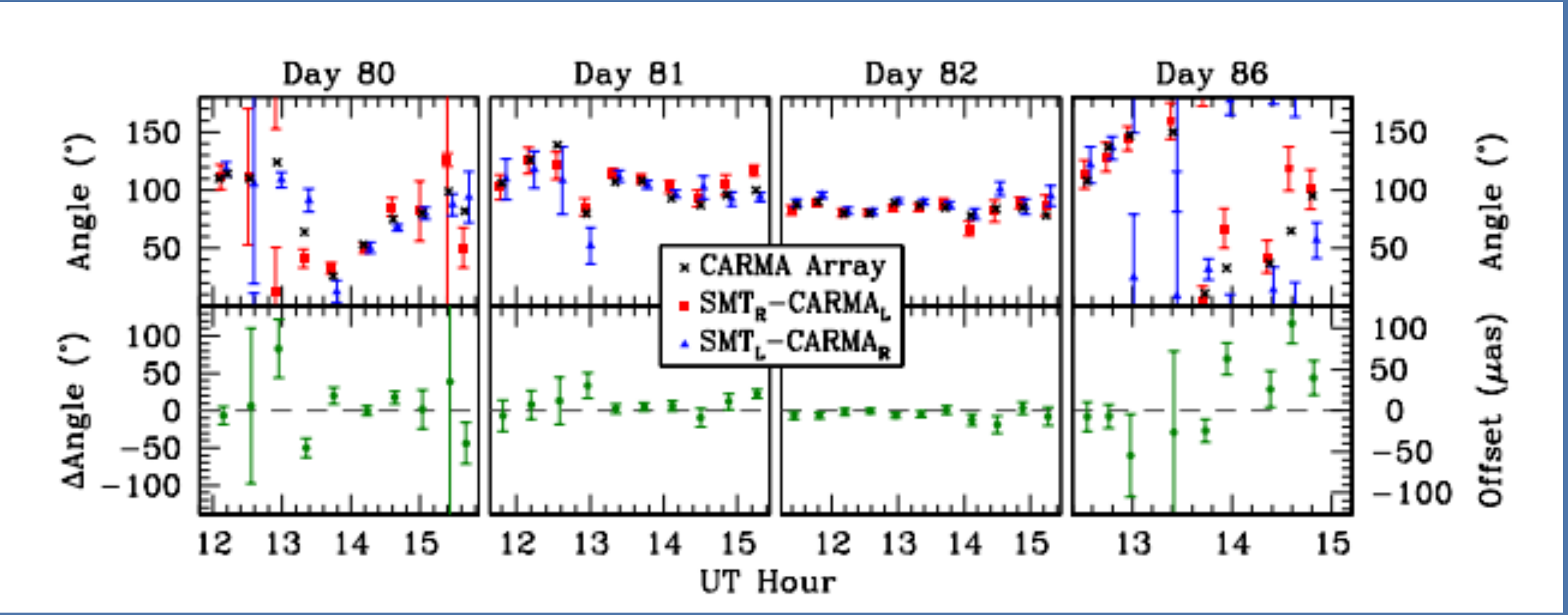

No spatial resolution

- M. D. Johnson et al., Science 350, no. 6265, 1242 (2015)

A subset of EHT has achieved at a precision of 3 degree!

-

BH superradiance

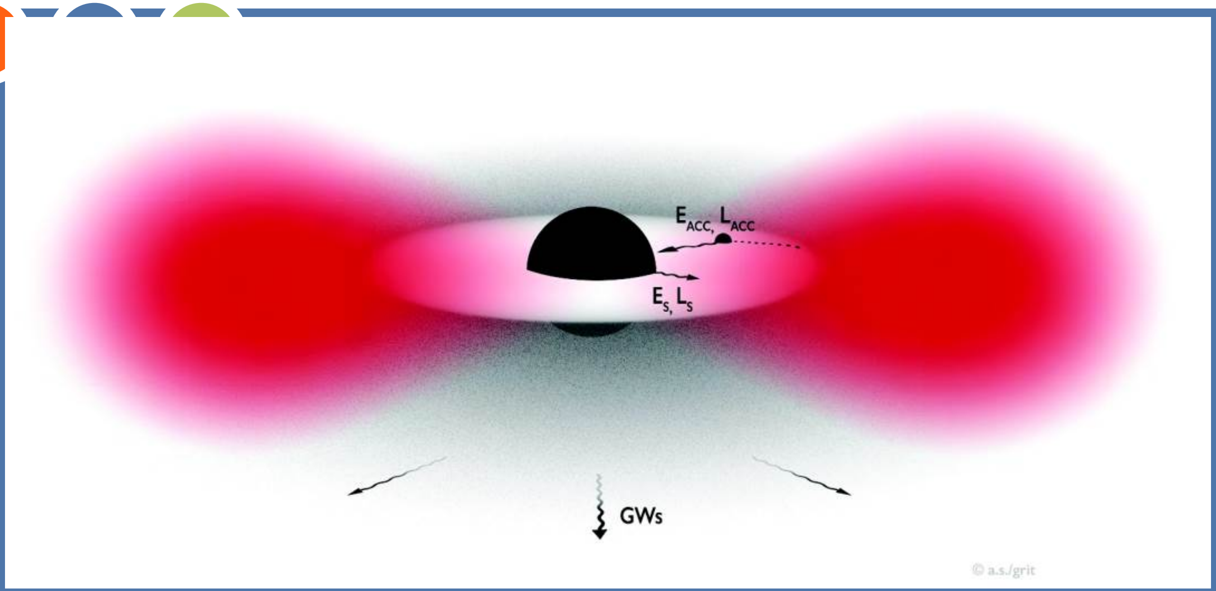

Superradiance condition

$$\omega < \omega_c = \frac{a_J m}{2r_+}$$

SR takes efficiently for the mass range

$$\frac{r_g}{\lambda_C} = \mu M \equiv \alpha \in (0.1, 1),$$

a rapidly rotating black hole loses:
energy + angular momentum

axion cloud will be produced around BH

energy in axion cloud can be comparable to BH mass!

BH superradiance

Axion cloud: Scalars in the Kerr backgrounds

Very similar to the hydrogen solution (non-relativistic limit):

$$a(x^\mu) = e^{-i\omega t} e^{im\phi} S_{lm}(\theta) R_{lm}(r)$$

$$\alpha \equiv \mu M$$

reduce to Y_{lm} in spherical
non-relativistic limit

$$\mathrm{Re}(\omega) \simeq \left(1 - \frac{\alpha^2}{2\bar{n}^2}\right)\mu$$

Imaginary part gives you the super-radiation

Axion cloud populates more efficiently at lower ℓ-mode.

$m=\ell$ mode is more efficient than other m-levels.

BH superradiance

Spatial distribution:

$$r_\pm = r_g \left(1 \pm \sqrt{1 - a_J^2}\right)$$

The ring from EHT has a radius comparable to the peaking radius of the axion cloud

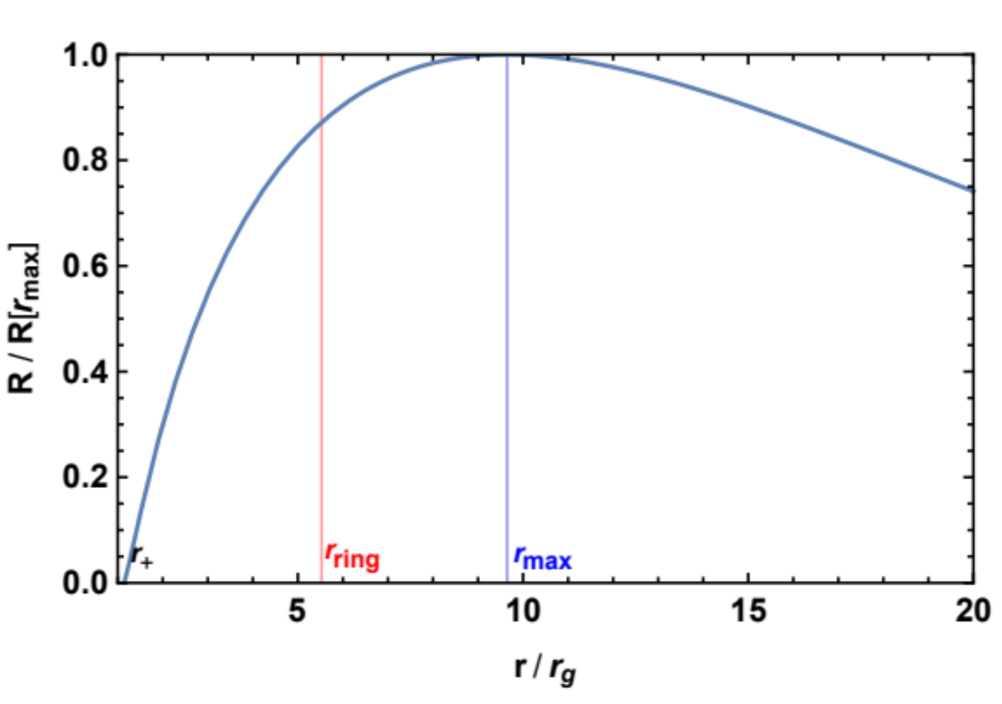

Axion cloud solution

Axion Lagrangian including self-interaction:

$$S = \int d^4x\sqrt{-g}[-\frac{1}{2}(\nabla a)^2 - \mu^2 f_a^2(1-\cos\frac{a}{f_a})]$$

K-G equation in the Kerr backgrounds

take

$$a = \frac{1}{\sqrt{2\mu}}(e^{-i\mu t}\psi + e^{i\mu t}\boxed{\psi^*})$$

slow varing function

gravitational potential

$$S_{\rm NR} = \int d^4x \left(i\psi^*\partial_t\psi - \frac{1}{2\mu}\partial_i\psi\partial_i\psi^* - \boxed{\frac{\alpha}{r}\psi^*\psi} + \boxed{\frac{(\psi^*\psi)^2}{16f_a^2}} \right)$$

self-interacting potential

Non-linear region

axion self-interaction becomes important when

gravitational potential ~ self-interacting potential

$$\frac{\alpha}{r} \simeq \frac{\mu a_0^2}{4 f_a^2}$$

Two possible consequences:

bosenova: a drastic process which explodes away axion cloud

steady axion outflow to infinity

numerical simulation has been performed:

H. Yoshino and H. Kodama, Prog. Theor. Phys. 128, 153 (2012), etc

Bosenova

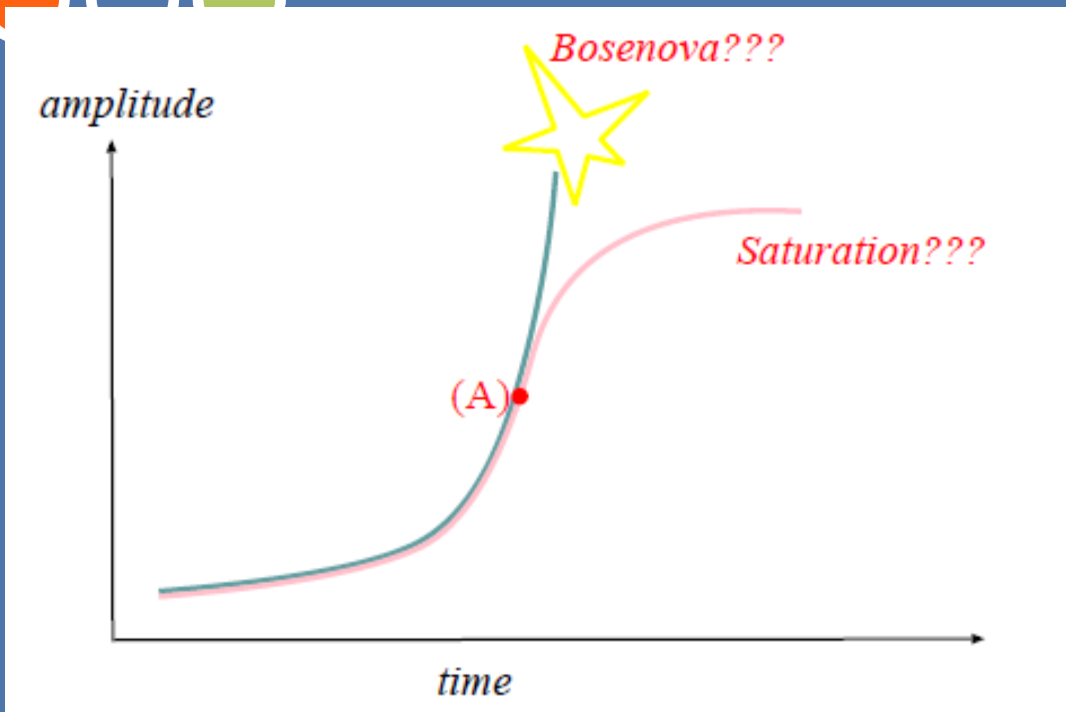

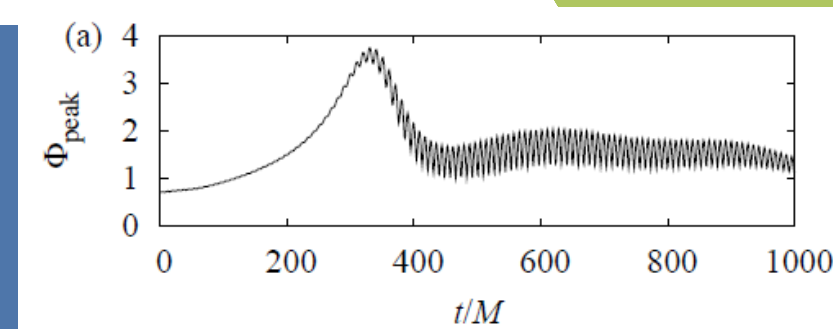

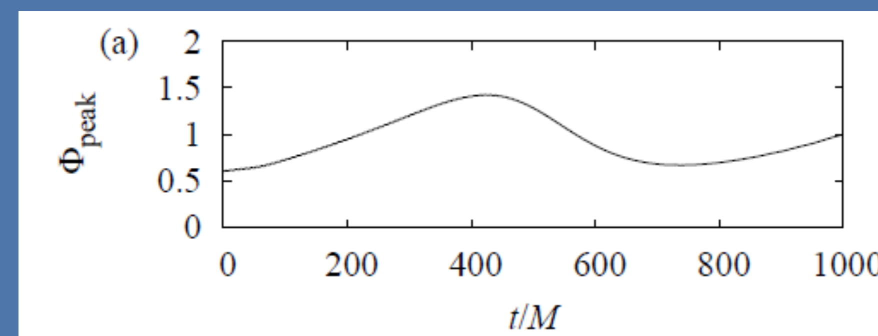

In either scenario, the amplitude of the axion cloud remains O(1) of its maximal value for most of the time

$$\frac{a}{f_a} \sim O(1)$$

The axion cloud stays after bosenova

Position angle change

Using $a_0 \approx f_a$ and $\omega \approx \mu$

Ignore axion density at earth

$$\Delta\Theta_{\rm max} \simeq -b g_{a\gamma} f_a \cos\left[\mu t_{\rm emit} + \beta(|\mathbf{x}_{\rm emit}| = r_{\rm max})\right],$$

$$b \equiv a_{max}/f_a$$

$$\Delta\Theta(t,r,\theta,\phi) \approx -\frac{b g_{a\gamma} f_a R_{11}(r)}{R_{11}(r_{\rm max})} \sin\theta \cos\left[\omega t - m\phi\right]. \quad (17)$$

Require both time and spatial resolution

additional loop suppression to translate f_a to axion-photon coupling

$$g_{a\gamma} \equiv \frac{c}{2\pi f_a} \equiv \frac{c_\gamma \alpha_{em}}{4\pi f_a},$$

fermion loop $c_\gamma \sim NQ^2.$

clockwork $c_\gamma \sim 2Q^2 q^{N-M}.$

Large

Polarmetric measurements

Requirements:

Concentration of axion: oscillating background fields

Stable (position angle) polarized source

Search for:

Position angle oscillate with time

Position angle oscillate with spatial distributions (extended source)

Polarmetric measurements at EHT from the axion cloud!

Position angle change

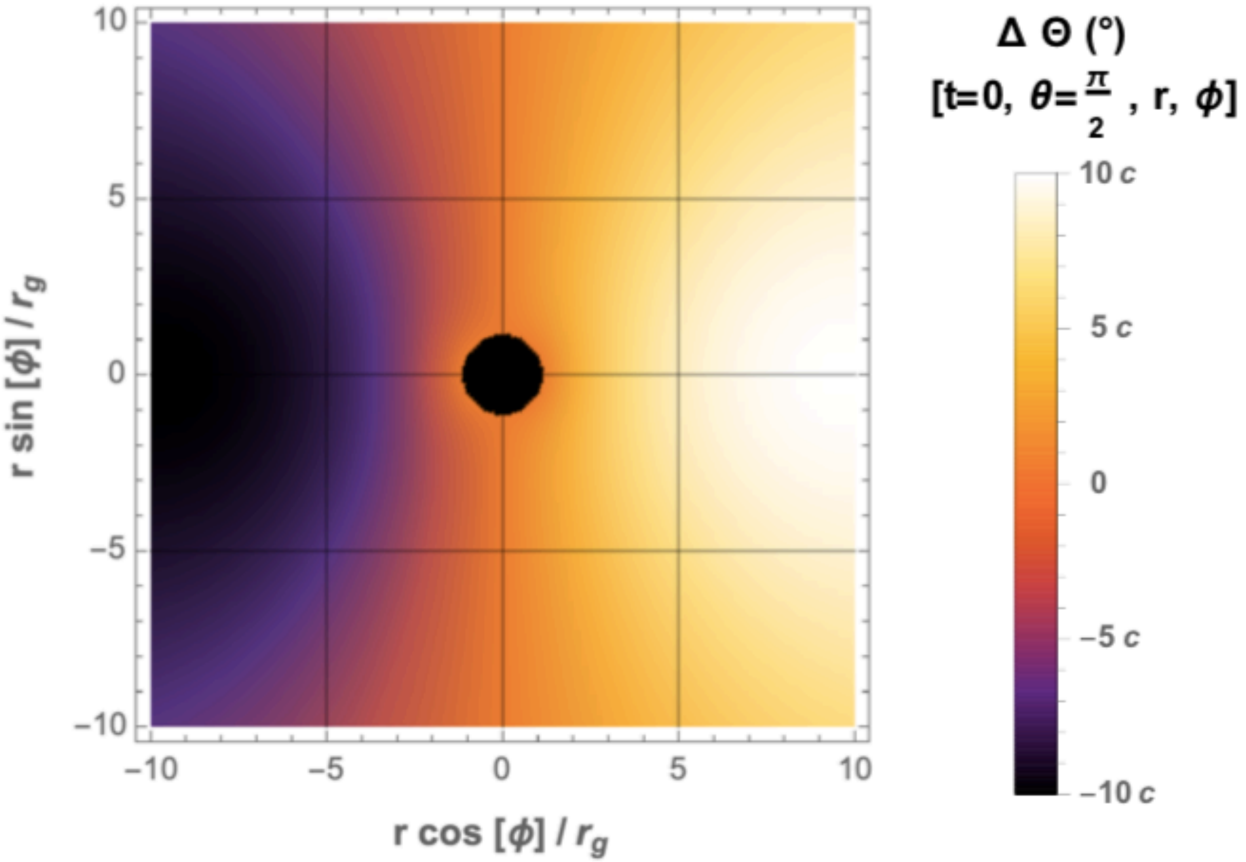

FIG. 2: $\Delta\Theta(t = 0, \theta = \pi/2, r, \phi)$ viewed along the rotating axis of the black hole. The amplitude of oscillation is around $8c^{\circ}$ at $r_{\rm ring}$ for $l = 1$, $m = 1$, $\alpha = 0.4$, and $a_J = 0.99$. The region of $r < r_+$ is masked.

- temporal dependence for a fixed position

- spatial dependence for a fixed time

Expected Limit

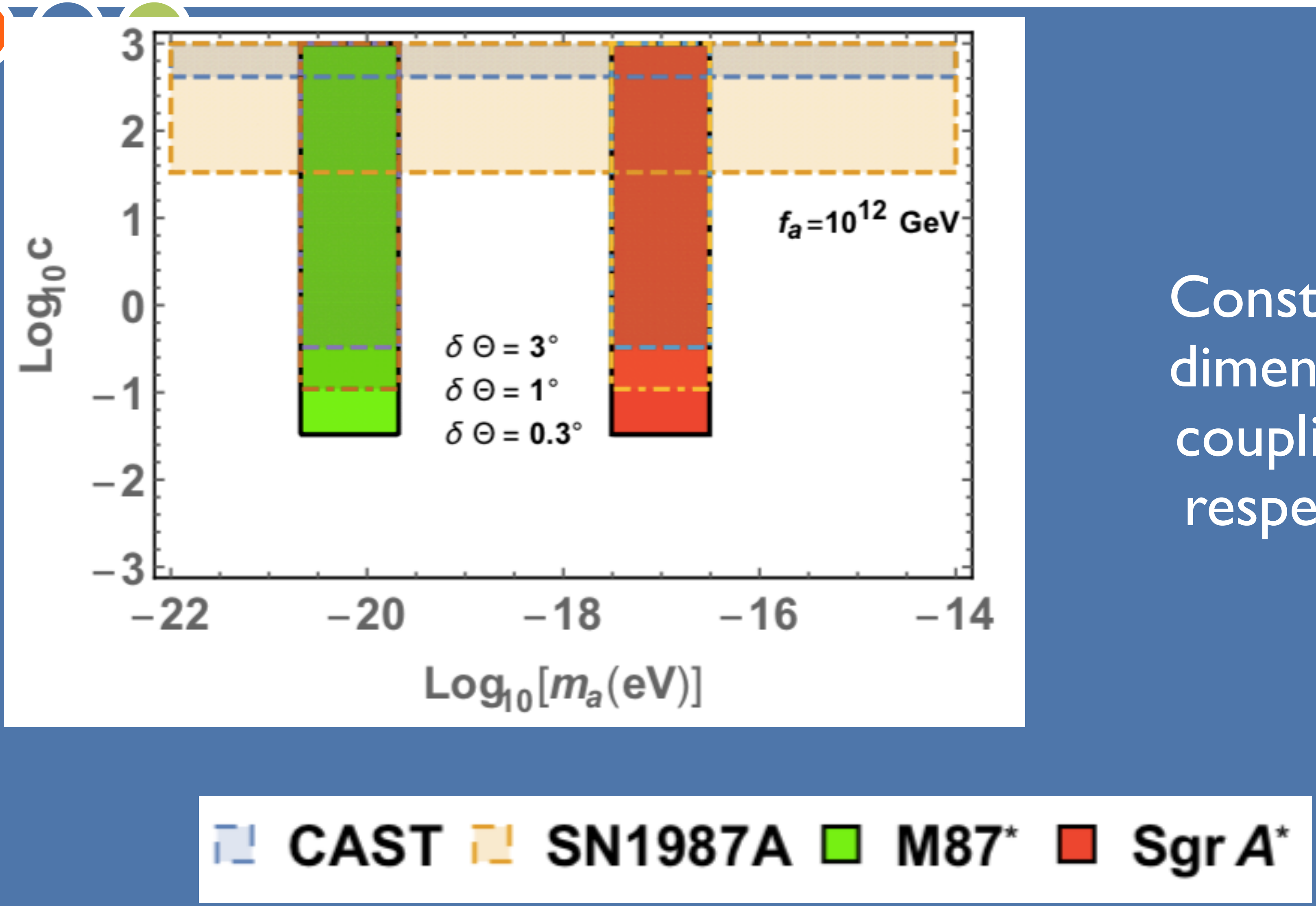

Constrain the dimensionless coupling with respect to fa

Summary

Ultra-light particles can form an oscillating background, cause extra forces on the observer and the objects we observe

Oscillating Velocity change: observed by Gaia

Arriving Time (pulse) change: observed by PTA Real data/better sensitivity

Supermassive Black holes provides excellent probes to search for axion!

A dense axion cloud can build up near by SMBHs.

Position angles varies when traveling through the axion cloud

Probe the existence of axion clouds by EHT.

Different than BH spin measurement. (Nonlinear region)

Different than other experiment. (dimensionless coupling)

Backup

TOA残差

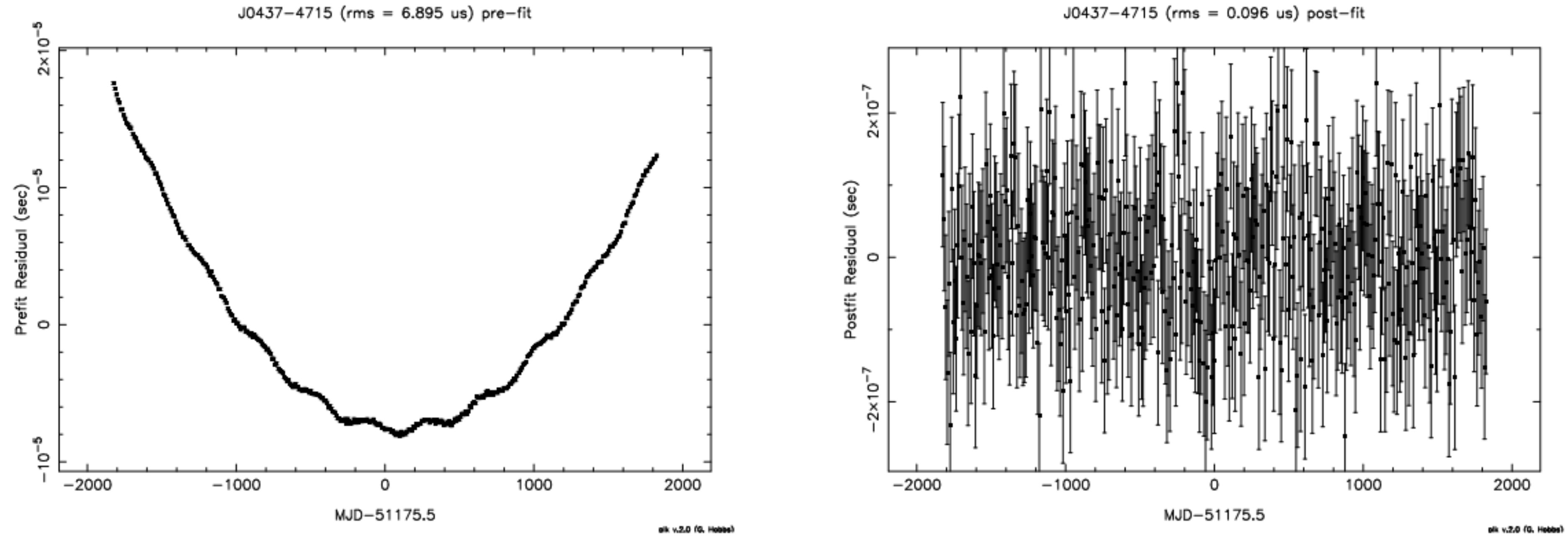

Figure 1: a) pre-fit timing residuals for the test data-set and b) post-fit timing residuals.